XX IMEKO World Congress
Metrology for Green Growth
September 9–14, 2012, Busan, Republic of Korea

ON THE USE OF SMART METERS FOR CONTINUOUS MONITORING OF SYSTEM IMPEDANCE

D.Gallo, C.Landi, M.Luiso

Dipartimento di Ingegneria dell'Informazione,
Seconda Università di Napoli, Aversa, Italy
{daniele.gallo@unina2.it}

Abstract: This paper analyzes the possibility of utilizing the measurement results made by smartmeters to decrease the number of customers affected by prolonged outages so increasing smart grid reliability. For this scope this paper proposes a continuous monitoring of system impedance so that it would be possible to detect the progressive degradation of some system component and to assert its localization with certain accuracy. The approach is based on theory developed for fault location and theory of synchrophasors. Some experimental results, obtained with the presented approach are reported.

Keywords: Smartmeter, impedance measurement, transmission line, lumped equivalent circuit, synchrophasor.

1. INTRODUCTION

Over the past several years, the promise of smart grids and their benefits has been widely publicized. Bringing updated technologies to power generation, transmission, and consumption, smart grids are touted to revolutionize electrical market and our way of electricity usage. Electrical utility across the world is trying to address numerous challenges, including generation diversification, optimal deployment of expensive assets, demand response, energy conservation, increase of quality of service and reduction of cost [1].

A preeminent task that smart grid technology can try to address is the reduction of the number of customers affected by prolonged outages so increasing system reliability. Traditional approach adopted versus abnormal conditions is basically reactive in nature, this means that some actions are performed only after a fault occurs and an outage has been detected. In this way, the utility acts presuming that nonfaulted feeder sections and alternative feeders are healthy and capable of carrying rated power flow. By the time a fault has occurred, substantial electrical and mechanical damage has been experienced by distribution lines and apparatus. This can result in extensive outages, substantial expensive equipment repair and replacement, and unsafe conditions for the public. Distribution system operators have no means today to evaluate the health and assess the condition of their distribution systems [2].

Some fault events are unpredictable (eg lightning), but in many other situations, failures are the result of a progressive degradation of some system component. In this case the electrical system keeps working for days or weeks in conditions that worsen progressively until the final failure occurs producing outage or visible effects [3]. At that time the utility carries out the repair. Great benefit in terms of reduction of time of outage and of maintenance cost can be obtained adopting information coming from smart meters in order to detect potentially dangerous situation or for forecast incoming failure.

For this scope this paper proposes a impedance monitoring system able to detect the progressive degradation of some system component and assert its localization with a certain accuracy. The approach is based on theory developed for fault location [4-5] but implemented by a smartmeter monitoring system that continuously estimates line impedance alerting on its rapid change or progressive increasing or decreasing. Consequently, the aim is to go toward predictive, targeted maintenance, enabled by smart meter technology.

2. BASICS OF IMPEDANCE MEASUREMENT

Electrical power system distribution can be made by complex interconnections (see fig. 1). But, for the scope of this measurement method it is possible to focus on a line that has two smart meters at its ends, as schematically depicted in fig. 2.

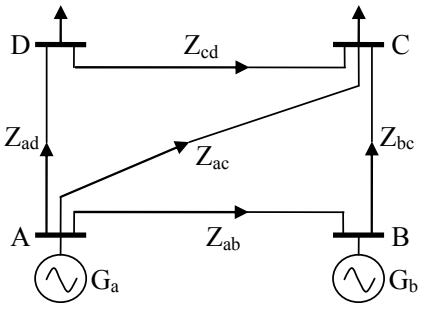

Fig. 1: Example of electrical connection system

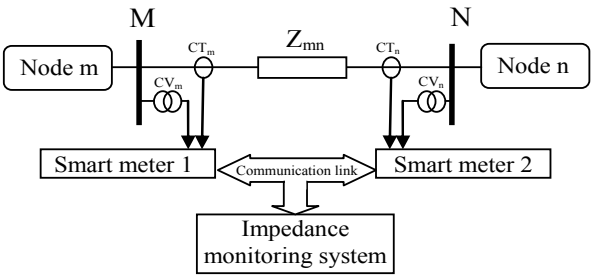

Fig. 2: Simplified diagram of two-end impedance measurement system

At each measurement node there are current transformers (CT) and voltage transformers (VT) which adapt level of signals to the measurement devices of smartmeters. Digital measurements are performed in each of these units for determining different kinds of quantity of interest (Active and reactive power, unbalance, harmonic pollution and interharmonic pollution, dip event monitoring, etc.). For the aim of this paper, attention is focused on a couple of smart meters that are charged with the task of carrying out impedance line monitoring. For this scope the A/D converters in the two smartmeters can perform the measurement independently (desynchronized measurement) or can refer to the same time reference (synchrophasors). In the first case the measurement results coming from the two meters can be combined to carry out a new measurement result only for specific purpose because the information about phase angle are incomparable as referred to different zero time reference. With synchrophasors also information on phase angle can be used. Usually for synchronization a GPS signal is used and the measurement system allowing synchronized measurement of the phasors of voltages and currents is referred to as the Phasor Measurement Unit (PMU) and is shown schematically in fig 3.

Obviously a smartmeter can be located at a power system node which different lines are connected to. In this case, it is able to monitor, at the same time, more than one line in collaboration with several other smartmeters and benefiting from the sharing of the same voltages for all the different impedance measurements.

As well know, under the assumption that the line is transposed (or symmetrical) and the voltage supply is balanced, each phase can be analyzed separately as two-terminal transmission line with distributed parameters. Generally, the distributed parameter circuit is used in the simulation as the model, especially for the research on traveling waves, but the corresponding line equation is very complex for calculation. In the practical analysis and calculation of power systems, under hypothesis of uniform characteristics, transmission line can be modeled as a two-port network, as schematically presented in Fig. 4

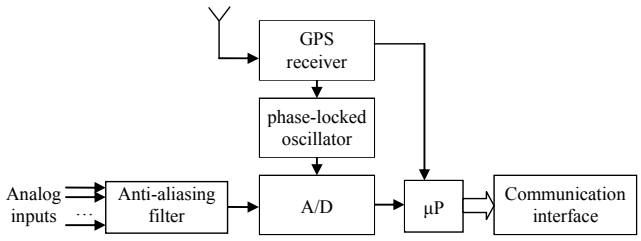

Fig. 3: Functional diagram of Phasor Measurement Unit (PMU)

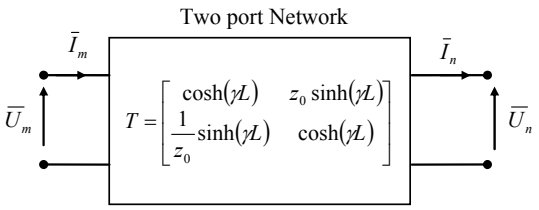

Fig. 4: Model of two-end power transmission system

The relation in steady state condition between voltage and current at the beginning (subscripts m) and the ending (subscripts n) of the line can be written as:

$$\begin{cases} \bar{U}_m = \bar{U}_n \cosh(\gamma L) + \bar{I}_n z_0 \sinh(\gamma L) \\ \bar{I}_m = \bar{U}_n \dfrac{1}{z_0} \sinh(\gamma L) + \bar{I}_n \cosh(\gamma L) \end{cases} \quad (1)$$

with

$$\begin{cases} \gamma = \sqrt{zy} = \sqrt{ZY}/L \\ z_0 = \sqrt{z/y} = \sqrt{Z/Y} \end{cases} \quad (2)$$

where L is the line length, z and y are respectively impedance and admittance per unit length and Z and Y are respectively total impedance and admittance of the line.

As for the application of the presented algorithm aimed to monitoring impedances on real power transmission line, in order to satisfy the hypothesis of balanced voltage supply in the following only the positive-sequence components are accounted. Nevertheless, more in general, from the measured signals can be extracted also [4-5]: i) incremental positive-sequence components; ii) negative-sequence components; iii) zero-sequence components. A comprehensive analysis of these aspects is beyond the scope of this paper.

Equation recalled in (1) allows to replace the transmission line with the π lumped parameter circuit that is reported in fig. 5. The lumped parameters can be easily obtained from (1) considering a short circuit at the second port ($\bar{U}_m = 0$), after same mathematical manipulation it results:

$$\begin{cases} Z'_{mn} = z_0 \sinh(\gamma L) = Z_{mn} \dfrac{\sinh(\gamma L)}{\gamma L} \\ Y'_{mn} = 2 \dfrac{\cosh(\gamma L) - 1}{z_0 \sinh(\gamma L)} = Y_{mn} \dfrac{\tanh(\gamma L/2)}{\gamma L/2} \end{cases} \quad (3)$$

where $\sinh(\gamma L)/\gamma L$ and $\tanh(\gamma L/2)/(\gamma L/2)$ are then the factors by which the total line series impedance and shunt admittance are to be multiplied in order to obtain the series impedance and shunt admittances of the equivalent π circuit. Also different circuit model exist but model π is more convenient for computational purposes [6].

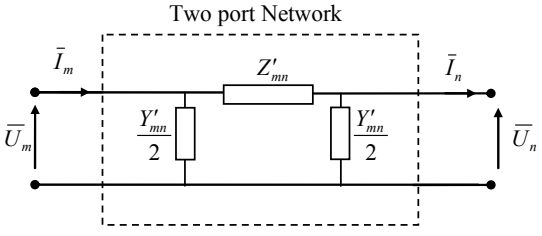

Fig. 5: Lumped model of two-end power transmission system

It should be emphasized that the π-equivalent circuit in fig. 5 is valid whatever the length of transmission line is and so, generally, parameters Z'_{mn} and Y'_{mn} are not equal to the total impedance and admittance of the line, Z_{mn} and Y_{mn}. However, for a typical power line (L<200 km) ,γL is small and the hyperbolic functions can be approximated with the argument as $\sinh(\gamma L) \approx \gamma L$ and $\tanh(\gamma L/2) \approx \gamma L /2$ these means that both correction factors approach to unity. A π-equivalent circuit in which the series arm has the impedance Z and each of the shunt arms has the admittance $Y_{mn}/2$, obtained by setting the correction factors equal to unity, is called a nominal π circuit. Substituting these values into (3), it gives the medium-length line (L between 80 and about 200 km) parameters

$$\begin{cases} Z'_{mn} = Z_{mn} \\ Y'_{mn} = Y_{mn} \end{cases} \tag{4}$$

Longer lines may be broken into two or more segments and each segment may be represented by a different π circuit. For a short-length line (L < 80 km) the charging current (and the capacitance C) may be neglected then the parameters become

$$\begin{cases} Z'_{mn} = Z_{mn} \\ Y'_{mn} = 0 \end{cases} \tag{5}$$

approaching to a scheme reported in fig. 5. Nevertheless, nowadays, with the wide use of high performance microcontroller, such approximations have limited practical value as the parameters can be easily calculated using (3) also for model like that reported in fig. 5.

Referring to circuit of fig. 5, it is possible to derive the relations among measurements results, obtained in steady state conditions at the two ports, that are able to carry out an evaluation of line impedance parameters. In fact, applying Kickoff low at currents that arrive to and departs from Z'_{mn}, it results

$$\bar{I}_m = \bar{I}_n + \overline{U}_m \frac{Y'_{mn}}{2} + \overline{U}_n \frac{Y'_{mn}}{2} \tag{6}$$

thus

$$Y'_{mn} = 2\frac{\bar{I}_m - \bar{I}_n}{\overline{U}_m + \overline{U}_n} = 2\frac{1 - \bar{I}_n / \bar{I}_m}{\overline{U}_m / \bar{I}_m + \overline{U}_n / \bar{I}_m} \tag{7}$$

Instead Ohm low applied to Z'_{mn} gives

$$\overline{U}_m - \overline{U}_n = \left(\bar{I}_m - \overline{U}_m \frac{Y'_{mn}}{2} \right) Z'_{mn} \tag{8}$$

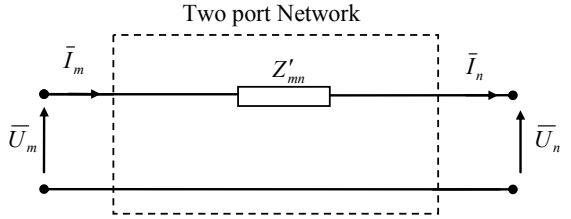

Fig. 6: Lumped model of short two-end power transmission system

Subsisting (7) in (8), after some mathematical manipulations it results:

$$Z'_{mn} = \frac{\overline{U}_m^2 - \overline{U}_n^2}{\overline{U}_m \bar{I}_n + \overline{U}_n \bar{I}_m} = \frac{\overline{U}_m / \overline{U}_n - \overline{U}_n / \overline{U}_m}{\bar{I}_n / \overline{U}_n + \bar{I}_m / \overline{U}_m} \tag{9}$$

Referring to circuit of fig. 6, a simpler relation can be derived, because obviously

$$\bar{I}_m = \bar{I}_n = \bar{I} \tag{10}$$

then (9) becomes

$$Z'_{mn} = \frac{\overline{U}_m - \overline{U}_n}{\bar{I}} = \frac{\overline{U}_m}{\bar{I}_m} - \frac{\overline{U}_n}{\bar{I}_n} \tag{11}$$

3. SYNCHROPHASOR REMARKS

Phasor Definition

A pure sinusoidal waveform can be represented by a unique complex number known as a phasor [7]. Consider a sinusoidal signal

$$x(t) = \sqrt{2} \cdot X \cdot \cos(\omega t + \varphi) \tag{12}$$

$$\overline{X} = X \cdot e^{j\varphi} = X \cdot [\cos(\varphi) + j \sin(\varphi)] = X_r + jX_i \tag{13}$$

The magnitude of the phasor, X, is the rms value of the sinusoid, and its phase angle, φ, is the initial phase angle of the signal so it is worthwhile underline that the value of φ depends on the time scale, particularly where t = 0. It is also important to note that phasor is defined for a specific angular frequency, ω, that is not explicitly stated in the phasor representation. This means that, in order to obtain coherent results, evaluation of other phasors must be done with the same time scale and frequency. The subscripts r and i in (13) signify real and imaginary parts of a complex value in rectangular components. Fig. 7 illustrates the relationship sinusoidal signal and its phasor representation.

The phasor in (13) is the synchrophasor representation of the signal x(t) in (12) if referred to the nominal system frequency and with zero time synchronized to UTC.

Voltage or current measurements, performed in two different sites within a large-scale distributed measurement system, such as that required for the proposed measurement task, in order to be correctly combined must to be carried out with the same zero-time reference and with reference to the same system frequency. This synchronization is usually obtained implementing synchrophasors (that is using GPS) but more in general also other synchronization techniques can be applied [8-11].

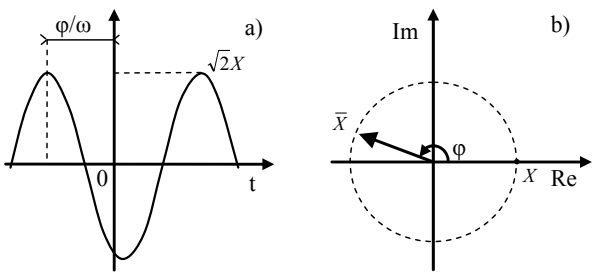

Fig. 7: (a) Sinusoidal signal, (b) Phasor representation.

Synchronization issues

For the following calculation two hypotheses are made

- all the phasor are referred to the same frequency;
- the system frequency is equal to the nominal value.

The first hypothesis refers to a steady situation for system frequency that is coherent the previous assumed hypothesis of stationary conditions. When the second hypothesis is not verified each phasor rotates at uniform rate, Δf, that is the difference between the actual and nominal frequency. This does not change the results that will be obtained in the following because the measured values are all expressed in the form of ratio between phasors (see (7), (9) and (11)). This implies that this common rotating component can be simplified and it does not appear in the result. For this reason it will not even be shown.

In order evaluate a measured quantity referring to different zero-time, the initial phase angles should be corrected with an additional phase angle, Δφ, that can be derived from time difference between to zero-time reference, τ, that is

$$\Delta\varphi = \omega\tau = 2\pi\frac{\tau}{T} \tag{14}$$

where T is system period, see fig. 8.

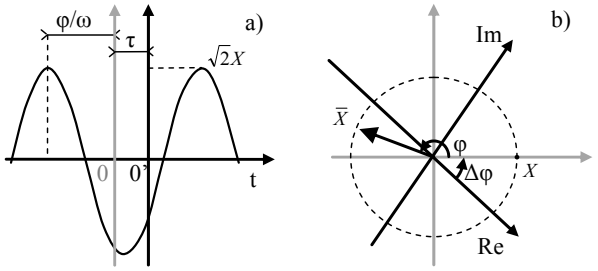

Fig. 8 Change of time zero-reference in (a) Sinusoidal signal (b) Phasor representation.

It is worthwhile evaluate what are the consequence of desynchronization for the obtained impedance measurement equations. For this aim let consider the phasor of voltage and current measured at first port

$$\overline{U}_m = U_m e^{j\alpha_m},\ \overline{I}_m = I_m e^{j\beta_m} \tag{15}$$

and the phasor of voltage and current measured at the second port

$$\overline{U}_n = U_n e^{j(\alpha_n+\Delta\varphi)},\ \overline{I}_n = I_n e^{j(\beta_n+\Delta\varphi)} \tag{16}$$

In this case an additional phase angle, Δφ, has been added to phase angle to account a possible desynchronization between measurements. The eq. (14) can be written as

$$Z'_{mn} = \frac{U_m e^{j\alpha_m}}{I_m e^{j\beta_m}} - \frac{U_n e^{j(\alpha_n+\Delta\varphi)}}{I_n e^{j(\beta_n+\Delta\varphi)}} = \frac{U_m}{I_m} e^{j(\alpha_m-\beta_m)} - \frac{U_n}{I_n} e^{j(\alpha_n-\beta_n)} \tag{17}$$

Thus

$$Z'_{mn} = Z_m - Z_n \tag{18}$$

It is apparent that the lack of synchronization does not produce any effect as the line impedance results from the difference of impedance seen independently from first and second port. This is a remarkable result that implies that the proposed algorithm applied to short line does not require synchronization between measurements. The accuracy of the results depends only on the accuracy in measurement of amplitude and difference of phase angle between current and voltage at each port.

Replacing (15) and (16) in (7) and (9) it results

$$Y'_{mn} = 2\frac{1 - I_n / I_m e^{j(\beta_n-\beta_m+\Delta\varphi)}}{U_m / I_m e^{j(\alpha_m-\beta_m)} + U_n / I_m e^{j(\alpha_n-\beta_m+\Delta\varphi)}} \tag{19}$$

$$Z'_{mn} = \frac{U_m / U_n e^{j(\alpha_m-\alpha_n-\Delta\varphi)} - U_n / U_m e^{-j(\alpha_m-\alpha_n-\Delta\varphi)}}{\bar{I}_n / U_n e^{-j(\alpha_n-\beta_n)} + I_m / U_m e^{-j(\alpha_m-\beta_m)}} \tag{20}$$

Assume a 10kV single phase transmission line which length L is equal to 200 km with per unit parameters: r = 0.17Ω/km, c = 0.00969μF/km, l = 1.21 mH /km.

The obtained relative deviations in measured impedance magnitude for different values of desynchronization phase angle, Δφ, is reported in fig. 9.

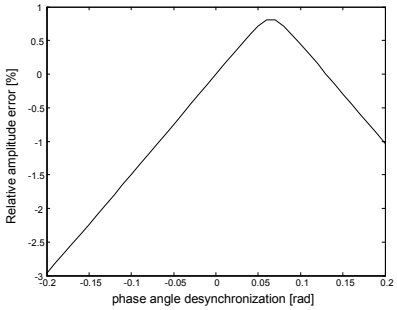

Fig. 9 relative deviation in measured impedance magnitude

4. EXPERIMENTAL RESULTS

In this section an experimental application of the described impedance monitoring system is presented.

The application pertains to the measurement of the impedance of a conductor rail (CR) in a subway tunnel under realization in the city of Naples, in the South of Italy. The length of the CR was approximately 700 m: in such conditions the line can be considered short and thus the model of Fig. 6, that is the lumped model of short two-end power transmission system, can be adopted for the CR in question.

The scope of the experimental test has been the measurement of the resistance and the inductance of the CR, when frequency changes.

The experimental setup consists in a power amplifier, an autotransformer with variable ratio, a waveform generator and a smart meter. The power amplifier is the Kepco 20-20 M, with output ranges of ± 20 V_{peak} for voltage and ± 20 A_{peak} for current, the frequency bandwidth is in the range of DC-50 kHz. As elevator autotransformer the Kepco ATB 15-200 has been employed: its input is in the range of ± 15 V_{peak}, its output in the range of ± 350 V_{peak} or ± 175 V_{peak} and the output power is 200 W. The waveform generator is the Agilent 33220A, with resolution of 14 bits, and generation frequency of 50 MHz. The smart meter is based on the ARM microcontroller STM32F103RB. The STM32 operates up to CPU clock speeds of 72MHz, it offers FLASH ROM sizes up to 128K (Program) and 20K SRAM (Data), Dual 12bit ADC with input range of 0÷3.3 V, general purpose timers, I^2C, SPI, CAN, USB and a

real-time clock. The utilized voltage and current transducers are, respectively, LEM LV-25 and LA-25: they are interfaced to the microcontroller through a conditioning circuit.

In Figure 10 the insertion of the measuring instruments is shown, while in Figure 11 and Figure 12 the curves, respectively, of resistance and inductance of the CR versus the frequency are represented. It can be seen that resistance increases with frequency while inductance decreases.

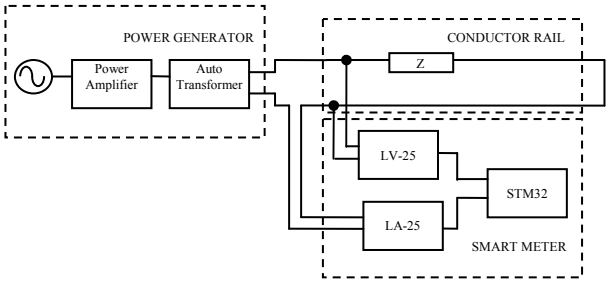

Figure 10. Insertion of the experimental setup.

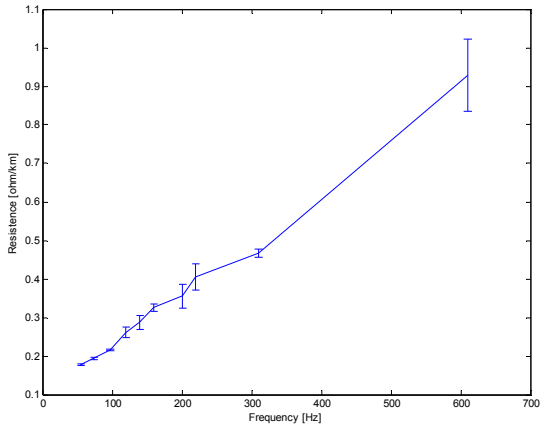

Figure 11. Resistance of the conductor rail vs. frequency.

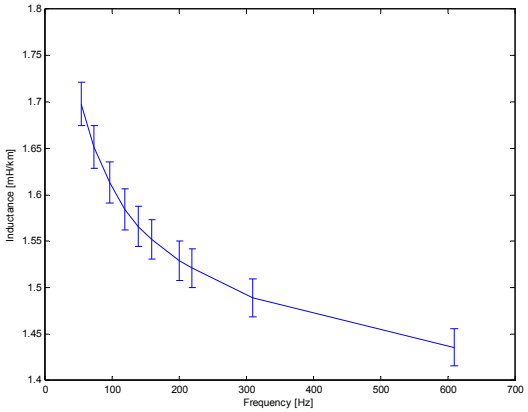

Figure 12. Inductance of the conductor rail vs. frequency.

5. CONCLUSIONS

This paper analyzes the possibility to utilize the measurement results made by smart meters to decrease the number of customers affected by prolonged outages so increasing smart grid reliability. For this scope this paper proposes a continuous monitoring of system impedance so that it would be possible to detect the progressive degradation of some system component and to assert its localization with certain accuracy. The approach is based on theory developed for fault location and theory of synchrophasors. Some experimental results, obtained with the presented approach are reported and they show the validity of the presented approach.

6. REFERENCES

[1] H. Farhangi, “The path of the smart grid”, IEEE Power and Energy Magazine, Vol. 8 , I. 1, 2010

[2] T. Flick, J. Morehouse “Securing the smart grid: next generation power grid security” 2011 Elsevier Inc.;

[3] B. D. Russell, C. L. Benner, “Intelligent Systems for Improved Reliability and Failure Diagnosis in Distribution Systems” IEEE Trans. On Smart Grid, vol. 1, n. 1, june 2010

[4] J. Izykowski, E. Rosolowski, P. Balcerek, M. Fulczyk, M. M. Saha, “Accurate Noniterative Fault Location Algorithm Utilizing Two-End Unsynchronized Measurements” IEEE Transactions on Power Delivery, vol. 25, no. 1, january 2010

[5] A.de Oliveira, G. Steynberg, “Secure protection against synchronous and asynchronous power swings” IEEE/PES Transmission and Distribution Conference, 2008

[6] S. Galli, T. Banwell “A Novel Approach to the Modeling of the Indoor Power Line Channel” IEEE Trans. on Power Delivery, vol. 20, no. 3, july 2005

[7] A. Carta, N. Locci, C. Muscas, “A PMU for the Measurement of Synchronized Harmonic Phasors in Three-Phase Distribution Networks”, IEEE Transactions on Instrumentation and Measurement, Vol. 58 , I. 10.

[8] “IEEE Standard for Synchrophasors Measurement for Power Systems”, IEEE Std. C37.118.1, 2011.

[9] J. De La Ree, V. Centeno, J.S. Thorp, A.G. Phadke, “Synchronized Phasor Measurement Applications in Power Systems” IEEE Trans. on Smart Grid, v. 1, n. 1, June 2010

[10] A.Carta, N.Locci, C.Muscas, S.Sulis, “A Flexible GPS-Based System for Synchronized Phasor Measurement in Electric Distribution Networks”, IEEE Transactions on Instrumentation and Measurement, Vol. 57 , I. 11

[11] S. Chakrabarti, E.Kyriakides, M.Albu, “Uncertainty in Power System State Variables Obtained Through Synchronized Measurements”, IEEE Transactions on Instrumentation and Measurement, Vol. 58, I. 8